SUPPORTING INFORMATION

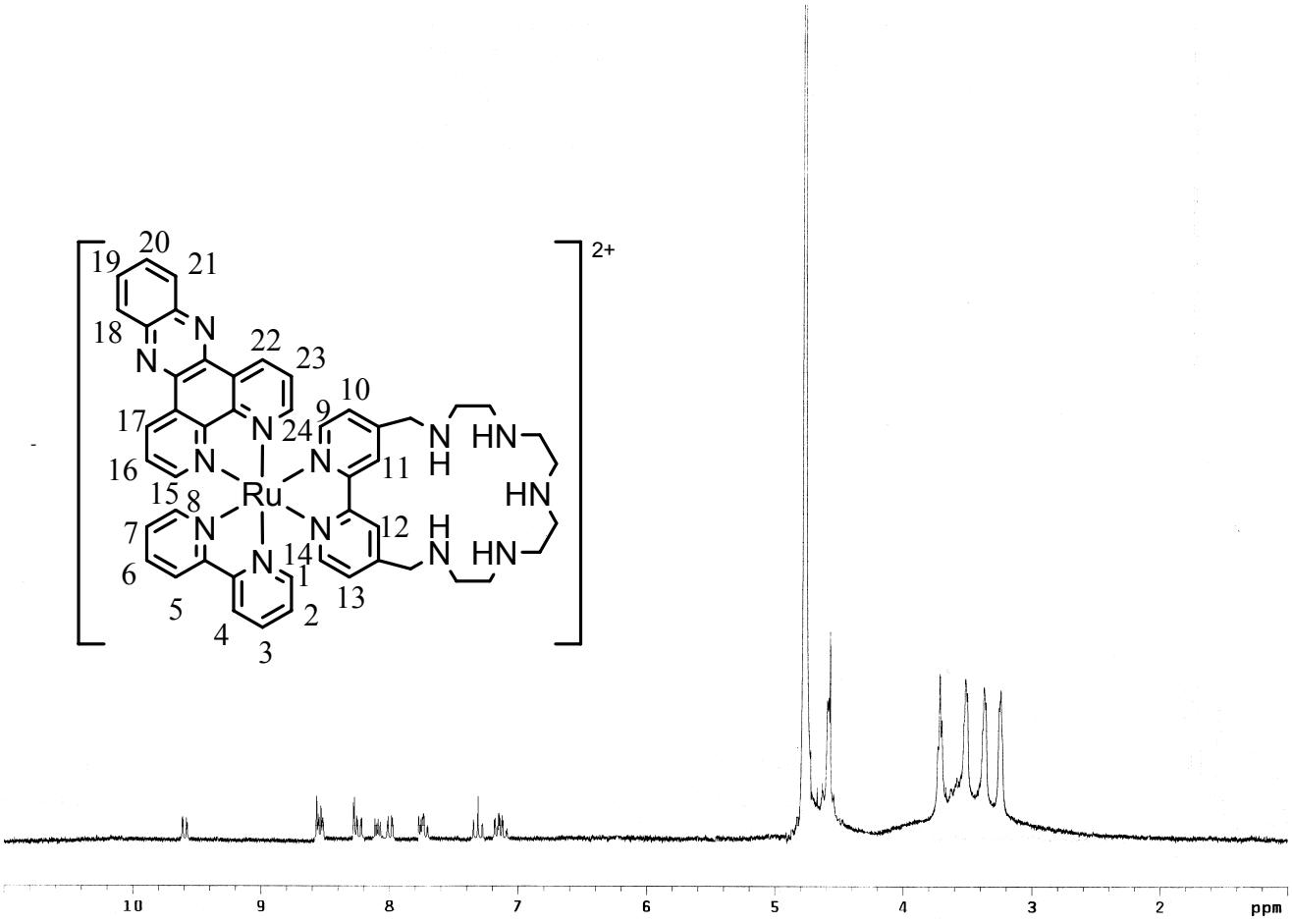

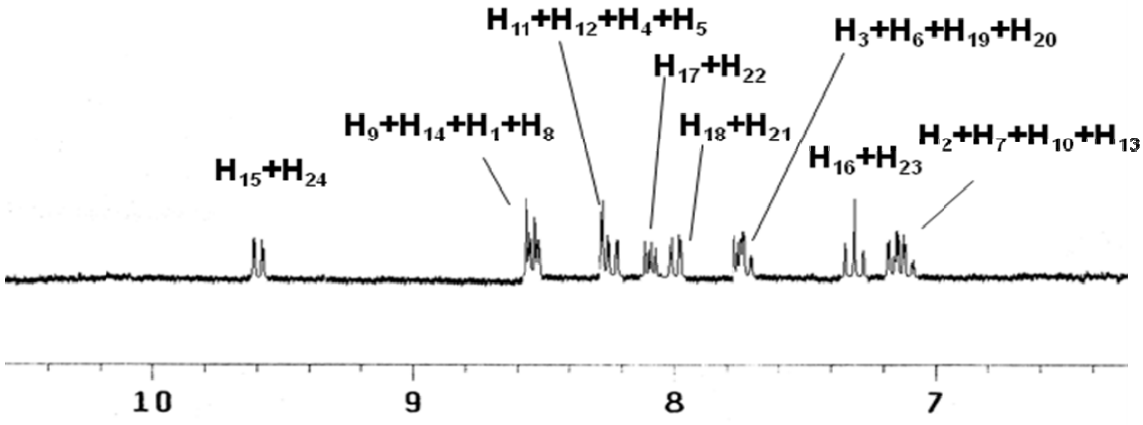

Figure S1. ^{1}H NMR spectrum of $D2^{2+}$ recorded in DMSO at 400 MHz

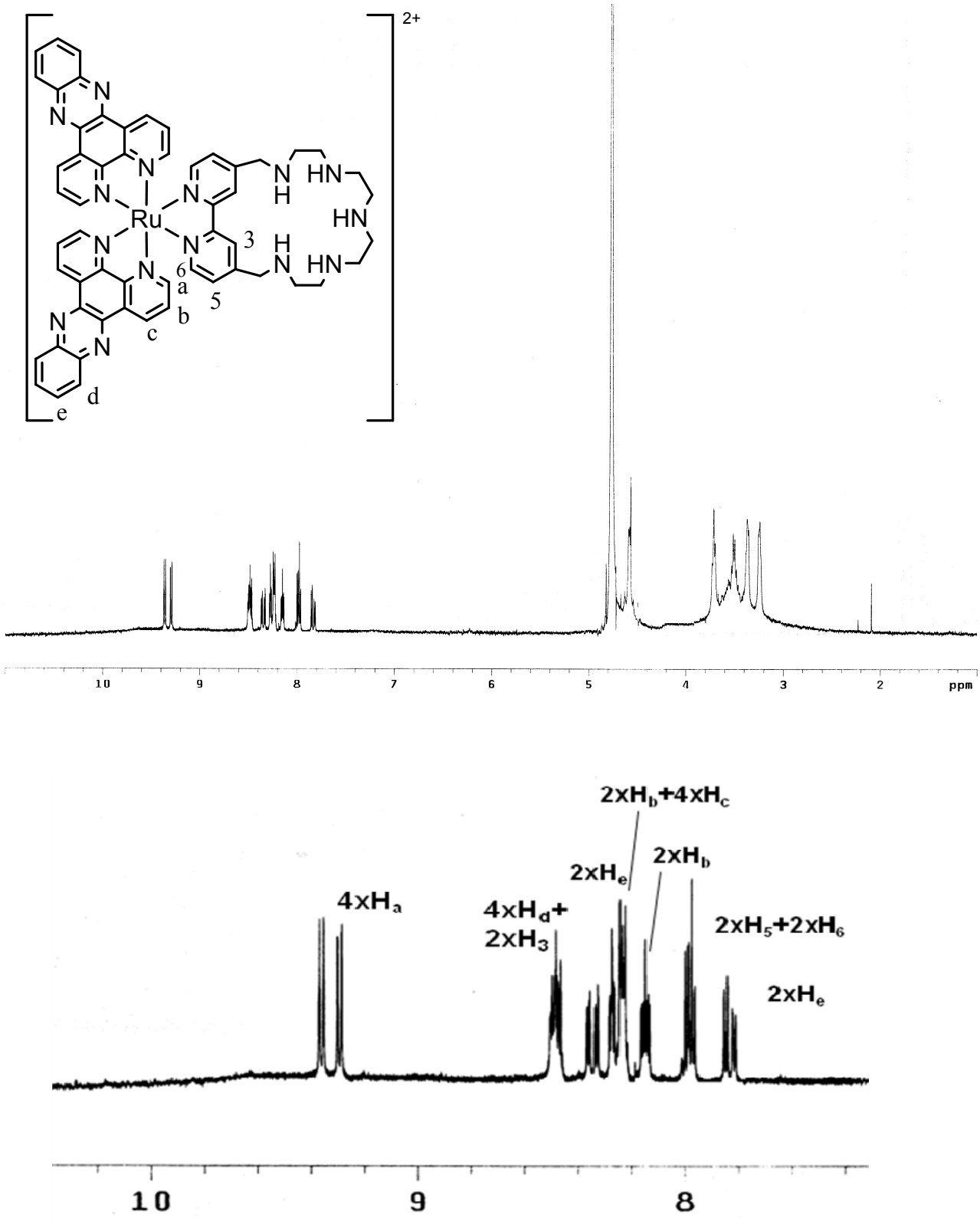

Figure S2. ^{1}H NMR spectrum of D3^{2+} recorded in DMSO at 400 MHz

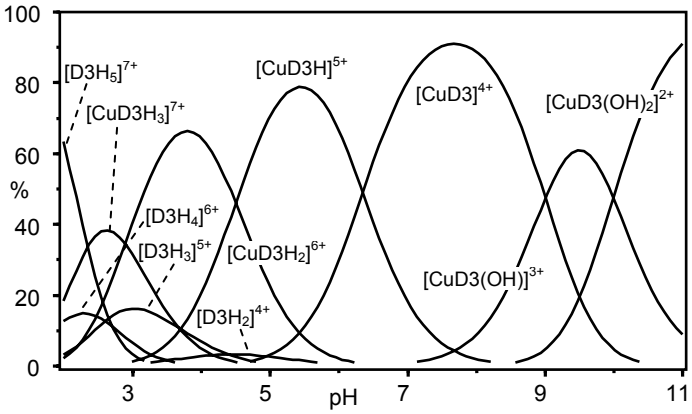

Figure S3. Distribution diagram of the Cu(II) complexes formed by $D3^{2+}$ in water. $[D3^{2+}] = [Cu(II)] = 1\times10^{-3}$.

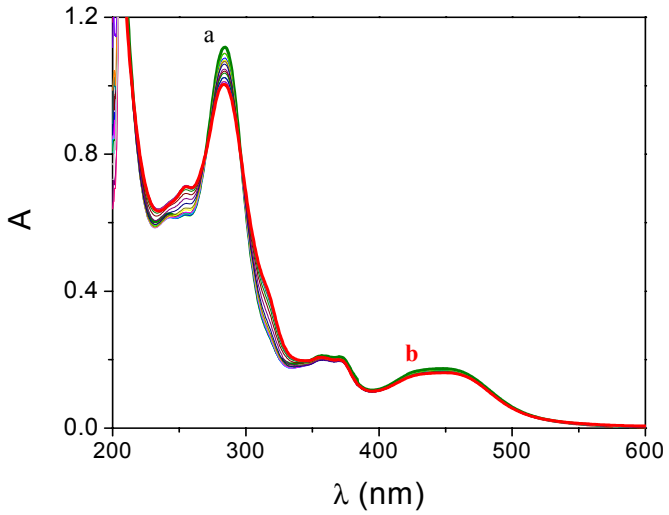

Figure S4. UV-Vis spectra for the $HD2^{3+}$ titration by copper(II). $C_{D2} = 1\times10^{-5}$ M, I = 0.10 M, pH = 7.0, T = 25°C, C_{Cu} = 0 M (**a**), 1.1×10^{-4} M (**b**).

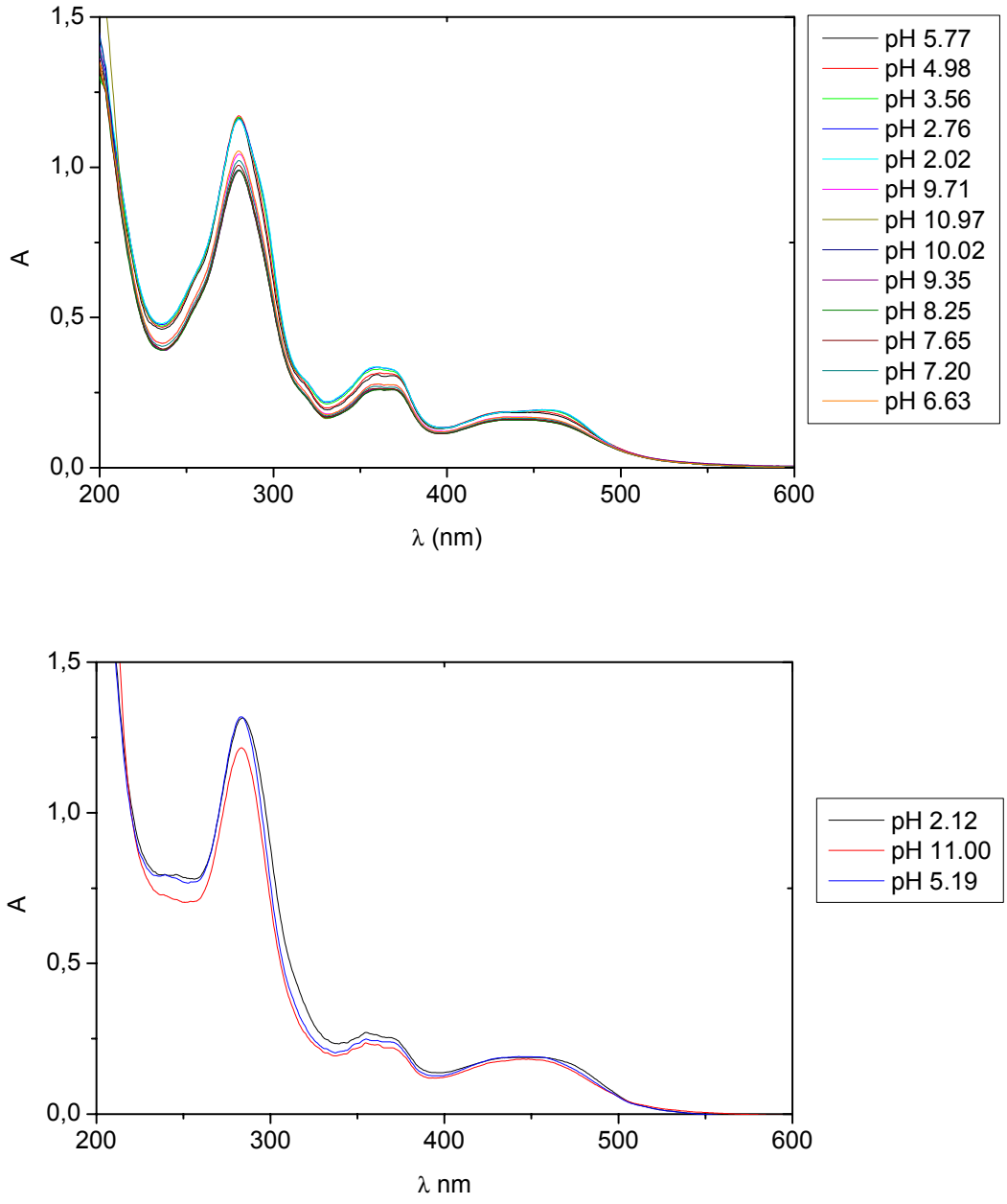

Figure S5. UV-vis absorption spectra of $D3^{2+}$ (a) and $D2^{2+}$ (b) recorded in water at different pH values and 25°C.

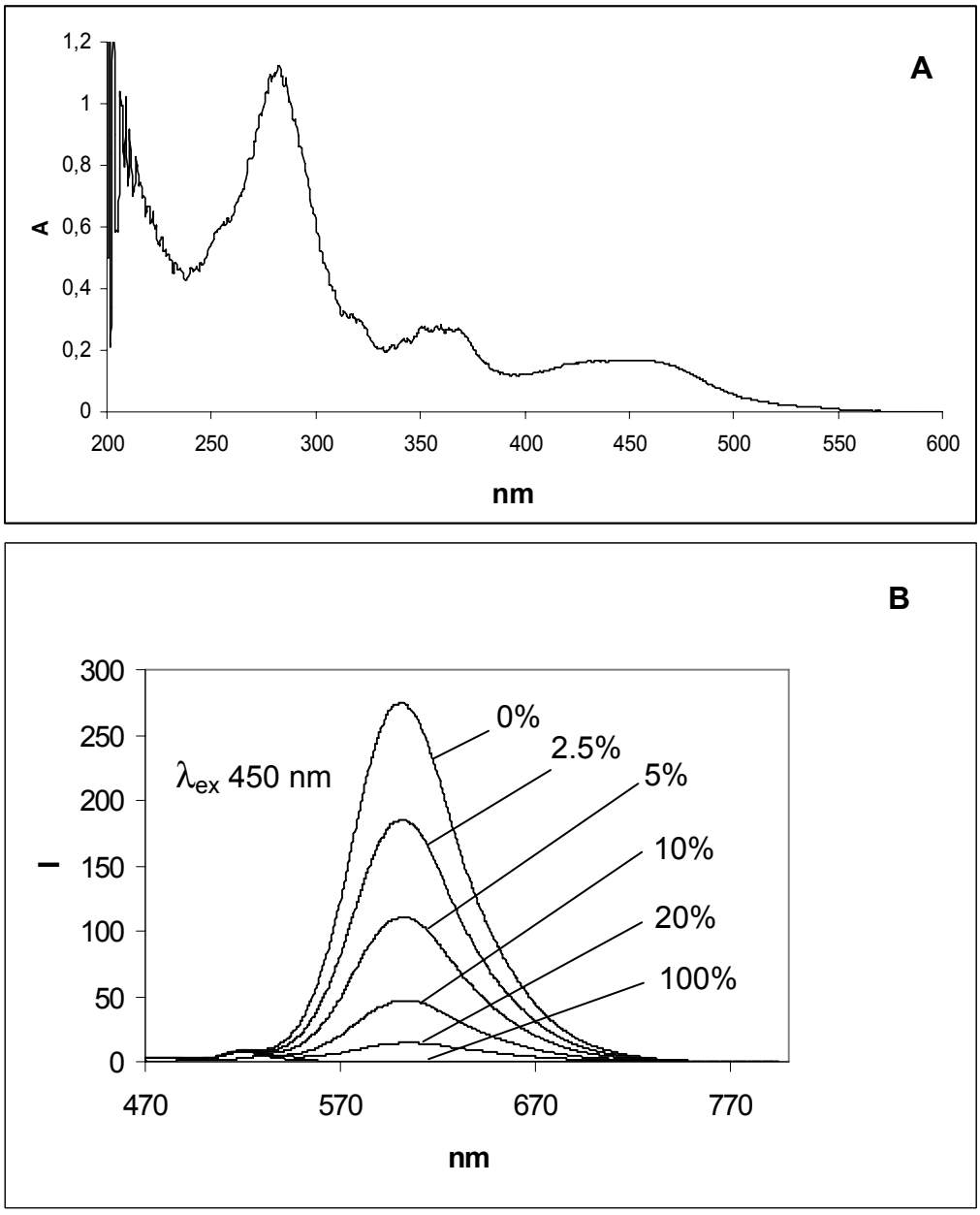

Figure S6. UV-Vis spectrum of $D3^{2+}$ in ethanol (A). Fluorescence emission spectra of $D3^{2+}$ in ethanol, water and ethanol/water mixtures (B). Percentages (v:v) are referred to water in ethanol. $[D3^{2+}] = 1\times10^{-5}$M, T = 25°C.

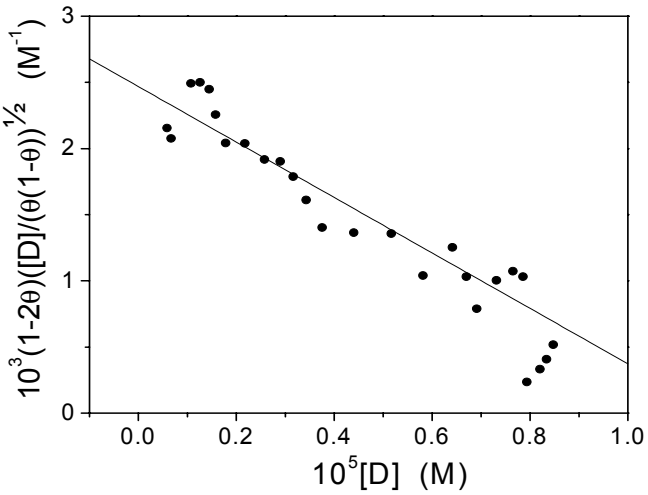

Figure S7. Analysis of fluorescence titration data for the DNA/CuD2^{4+} system to equation (6). I = 0.10 M, pH = 7.0, T = 25°C.

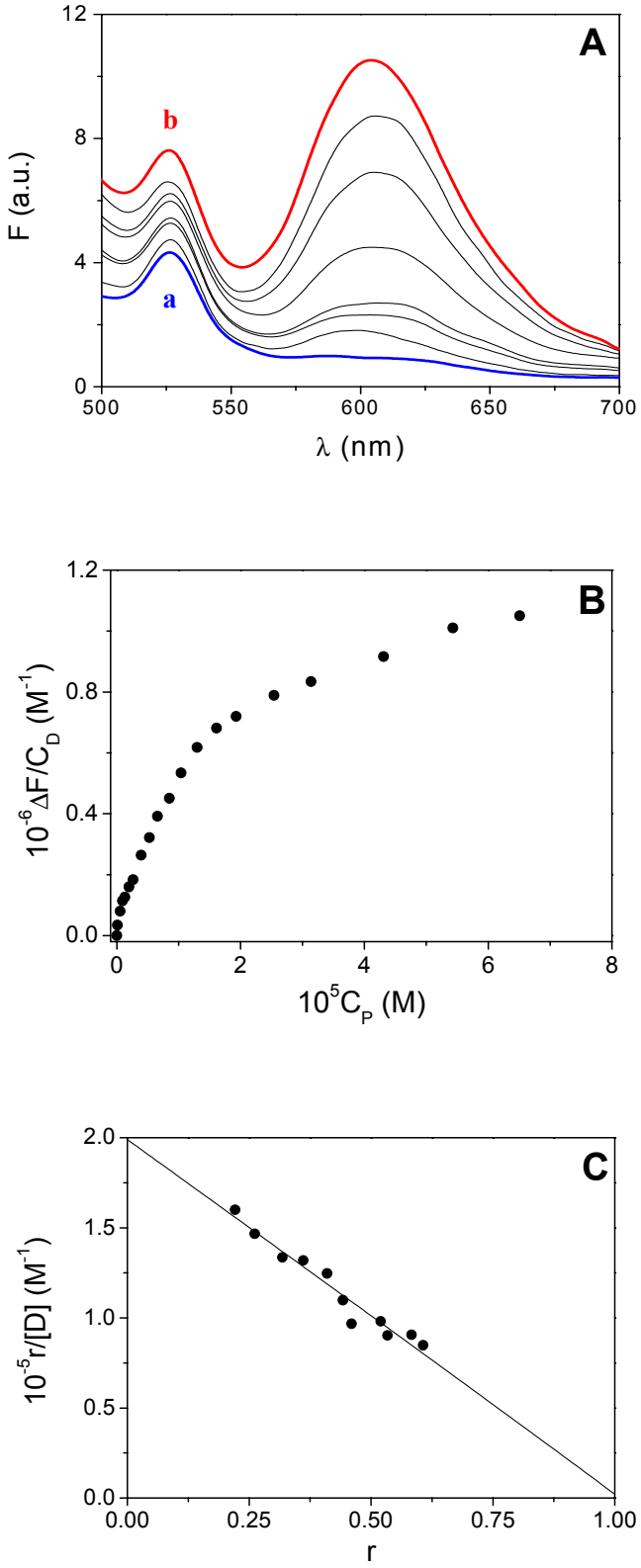

Figure S8. Spectrofluorometric titration of the DNA/HD3^{3+} system (A), relevant binding isotherm at λ_{em} = 600nm (B) and analysis of the fluorescence titration data to equation (5) (C). $C_D = 8.8\times10^{-6}$ M, C_P from 0 (**a**) to 6.5×10^{-5} M (**b**), λ_{ex} = 450nm, I = 0.10 M, pH = 7.0, T = 25°C.

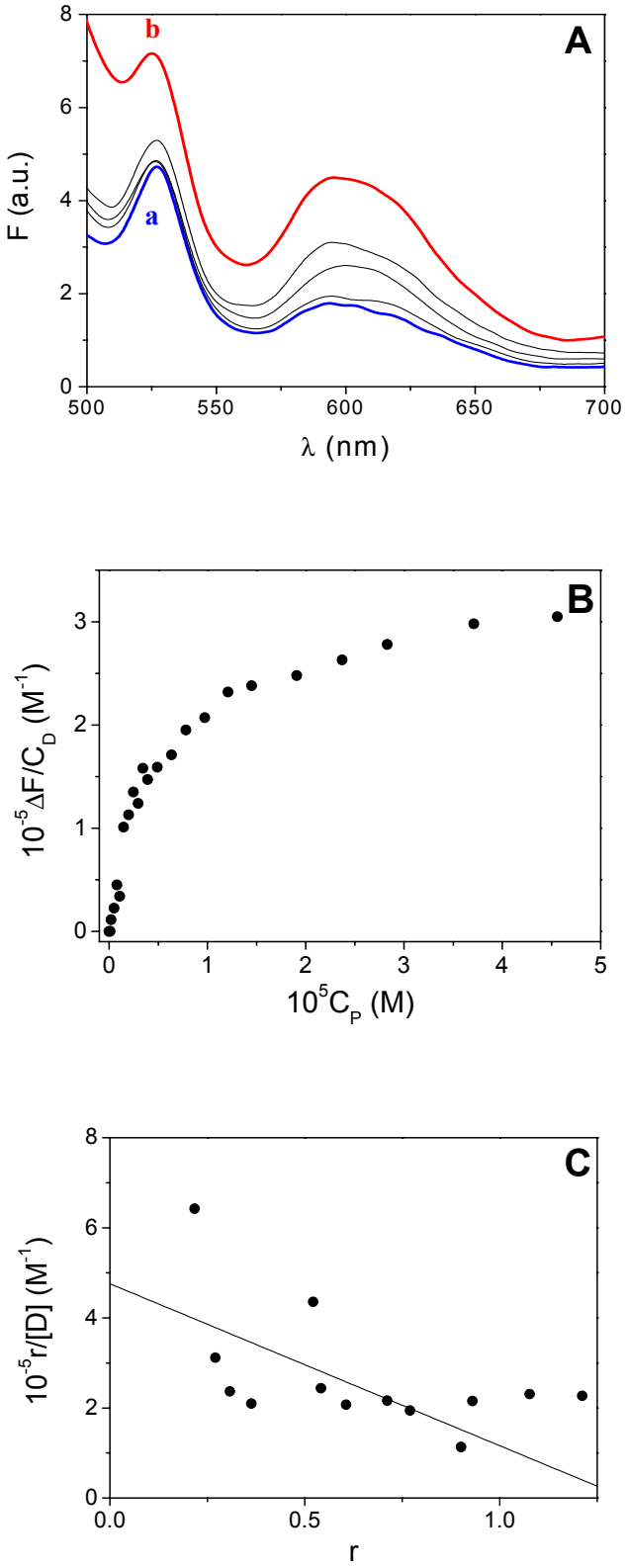

Figure S9. Spectrofluorometric titration of the DNA/CuD3^{4+} system (A), relevant binding isotherm at λ_{em} = 600nm (B) and analysis of the fluorescence titration data to equation (5) (C). $C_D = 8.8\times10^{-6}$ M, C_P from 0 (**a**) to 4.6×10^{-5} M (**b**), λ_{ex} = 450nm, I = 0.10 M, pH = 7.0, T = 25°C.

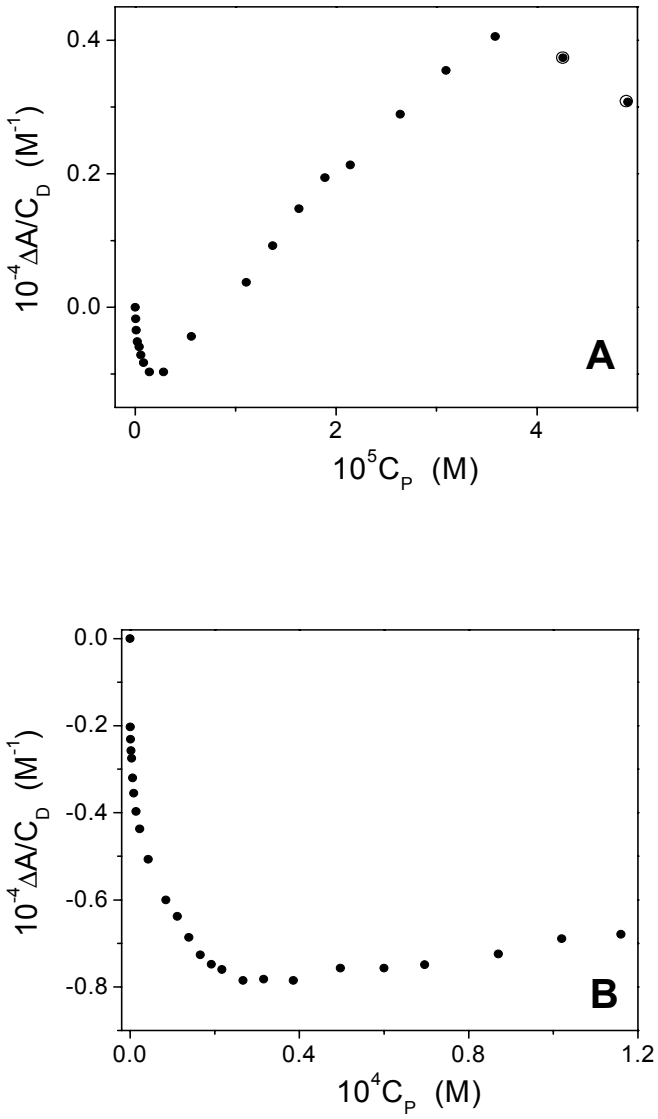

Figure S10. Binding isotherms from spectrophotometric titrations of the DNA/HD2^{3+} (A) and DNA/HD3^{3+} (B) systems under low added salt conditions; $C_D = 1.1\times10^{-5}$ M, I = 0.003 M, pH = 7.0, λ = 360 nm, T = 25°C. Circled points in (A) are related to precipitation phenomena.

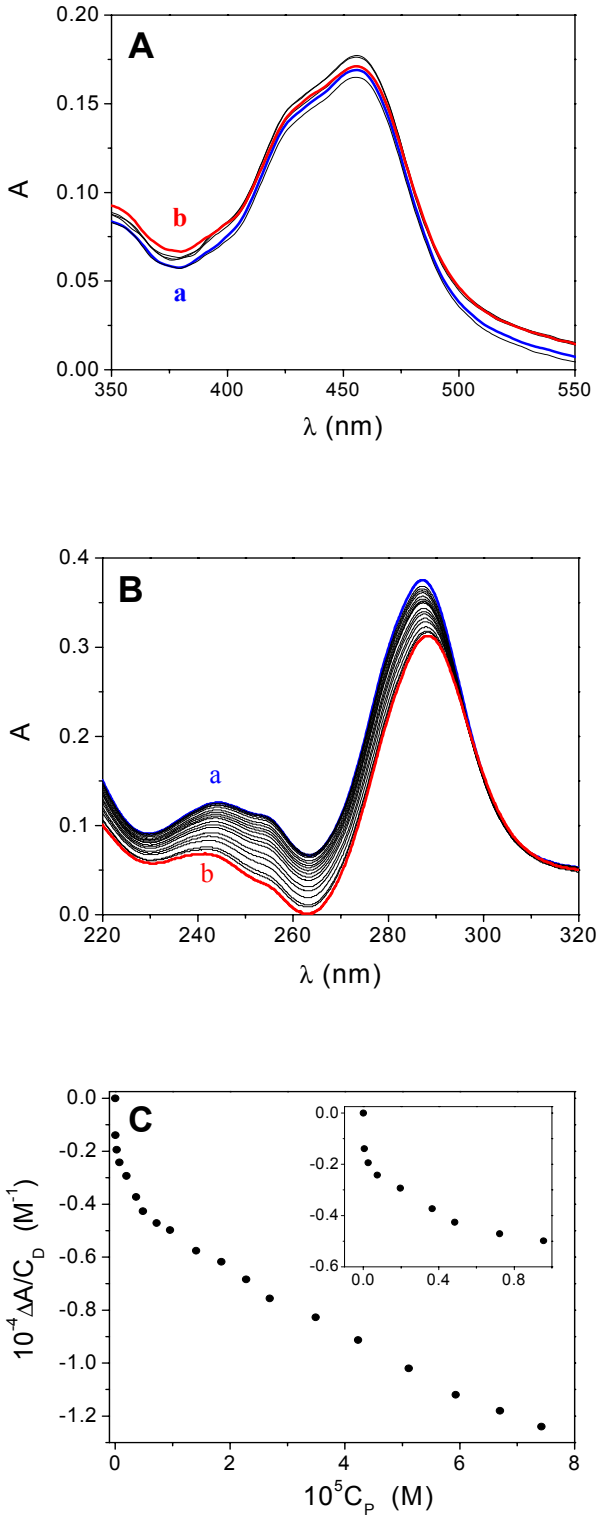

Figure S11. Spectrophotometric titrations of the DNA/H_2D1^{4+} system; I = 0.10 M, pH = 7.0, T = 25°C. (A) Visible range: $C_D = 1.2\times10^{-5}$ M, C_P from 0 (**a**) to 1.0×10^{-4} M (**b**). (B) UV range: $C_D = 5.0\times10^{-6}$ M, C_P from 0 M (**a**) to 7.4×10^{-5} M (**b**), differential titration (DNA added in both sample and reference cells). (C) Binding isotherm at 288nm from titration (B); the inset is an enlargement of the first part of the plot.

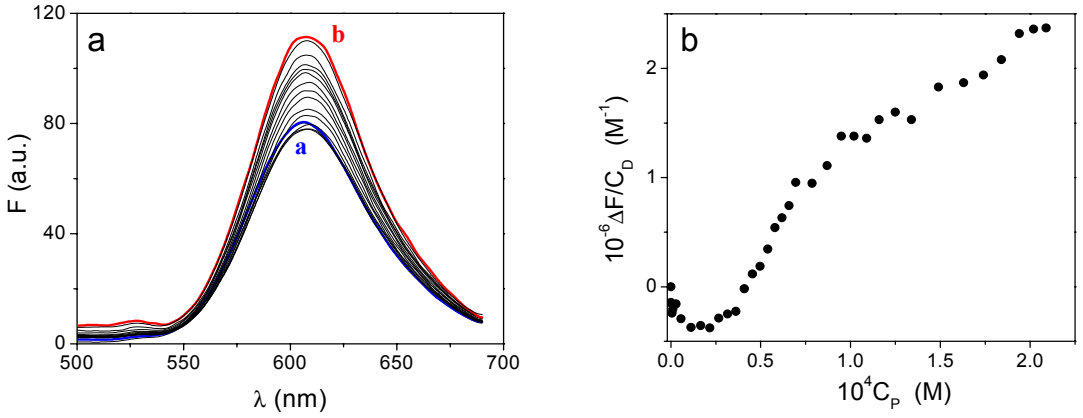

Figure S12. Fluorescence spectra for the DNA/H_2D1^{4+} system recorded during titration (a) and relevant binding isotherm at 607nm (b). $C_D = 1.2\times10^{-5}$ M, I = 0.10 M, pH = 7.0, T = 25°C, λex = 450nm, $C_P = 0$ M (a), 2.1×10^{-4} M (b).

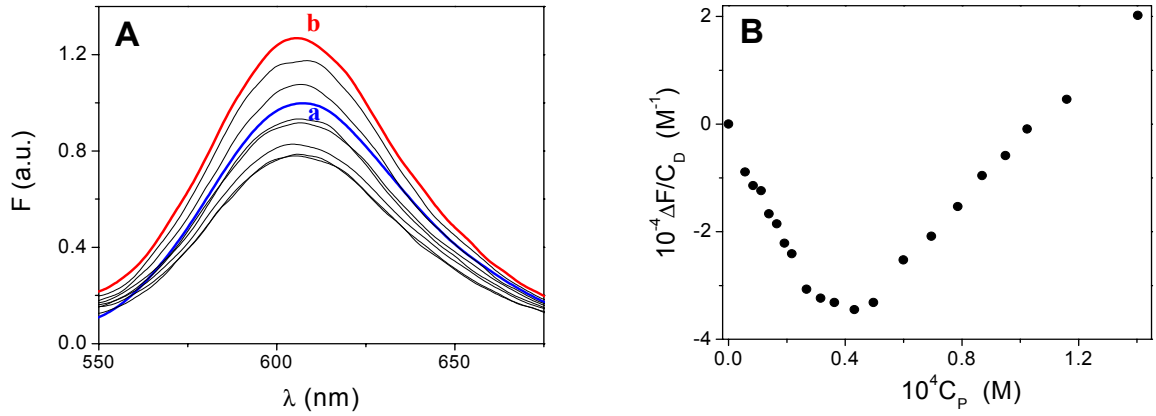

Figure S13. Spectrofluorometric titration of the DNA/CuD1^{4+} system; I = 0.10 M, pH = 7.0, λ_{ex} = 450 nm, T = 25°C. (A) Collected spectra $C_D = 1.3\times10^{-5}$ M, C_P from 0 (**a**) to 1.4×10^{-4} M (**b**). (B) Binding isotherm at λ_{em} = 607 nm.

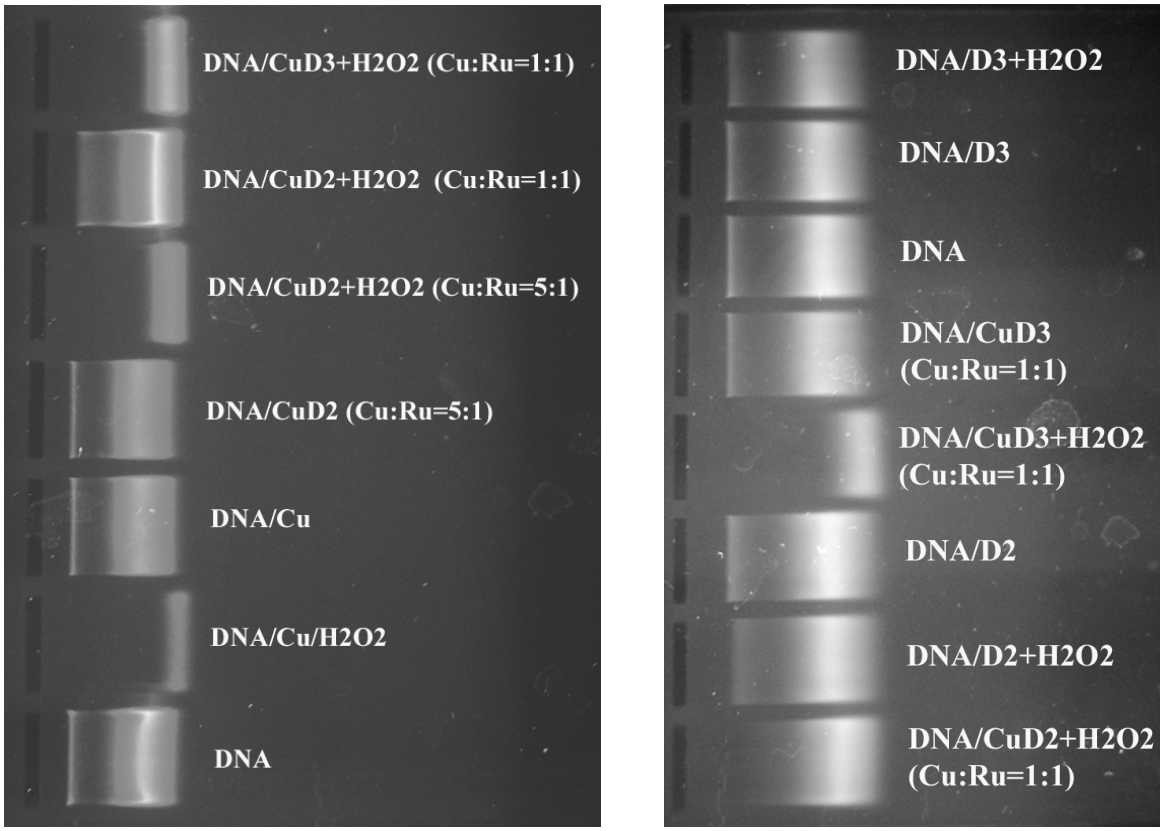

Figure S14. Electrophoresis experiments on the DNA/HD2^{3+}, DNA/CuD2^{4+}, DNA/HD3^{2+} and DNA/CuD3^{4+} systems, alone or in the presence of H_2O_2 (1.8×10^{-3}M). C_{DNA} = 2.5×10^{-4}M, Tris-acetate-EDTA buffer (pH = 7.4), 1% agarose gel with 1×10^{-6}M Ethidium staining, 65V, 50mA.

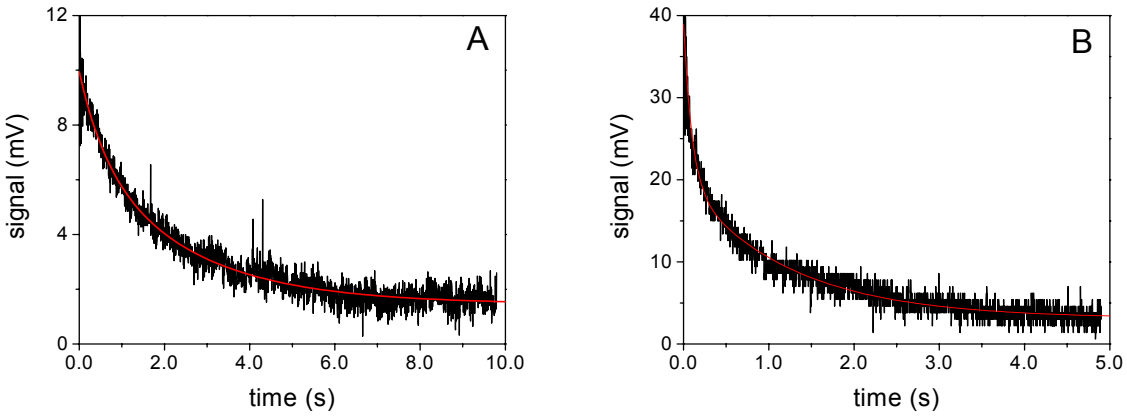

Figure S15. Stopped-flow curves for the DNA/HD2^{3+} system (A) and for the DNA/HD3^{2+} system (B) at I= 0.10 M, pH = 7.0, λ = 360nm, T = 25°C; the line is least-square bi-exponential data fitting. (A) $C_D = 9.4\times10^{-6}$ M, $C_P = 9.5\times10^{-5}$ M; (B) $C_D = 1.0\times10^{-5}$ M, $C_P = 2.0\times10^{-4}$ M.

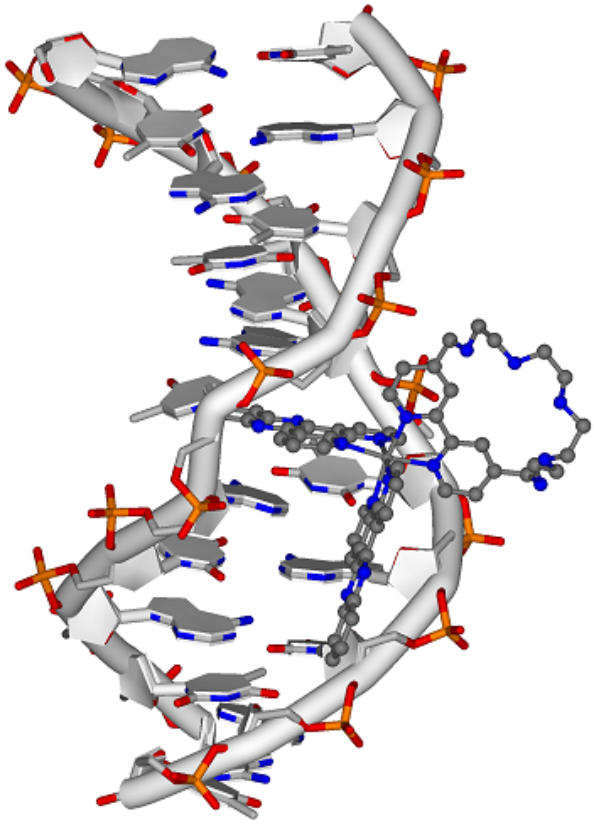

Figure S16. Calculated conformation for the ATATATATAT/Δ-HD3^{3+} adduct.

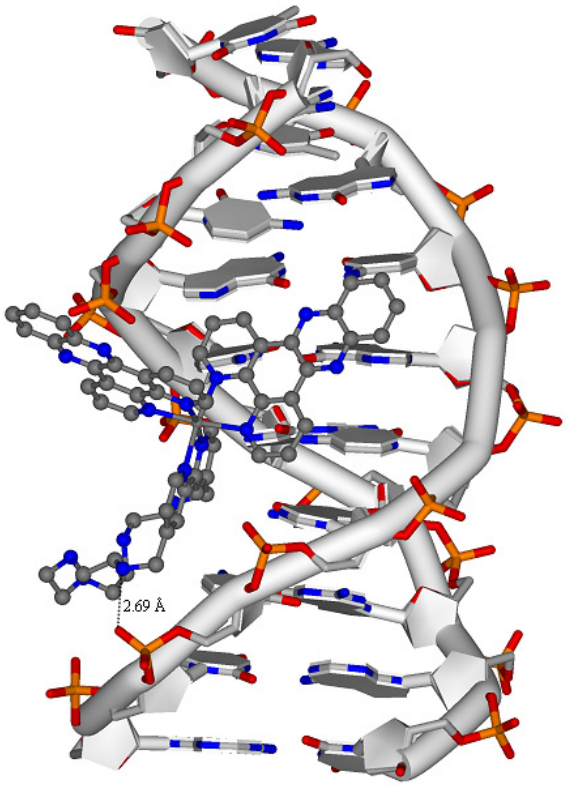

Figure S17. Calculated conformation for the ATCGCGCGAT/Λ-HD3^{3+} adduct.

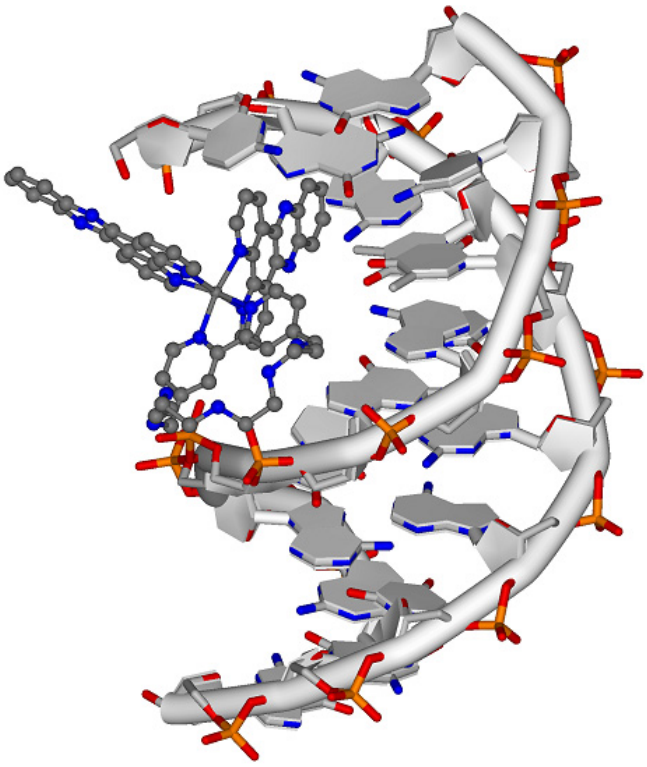

Figure S18. Calculated conformation for the CGATCGATCG/Δ-HD3^{3+} adduct.

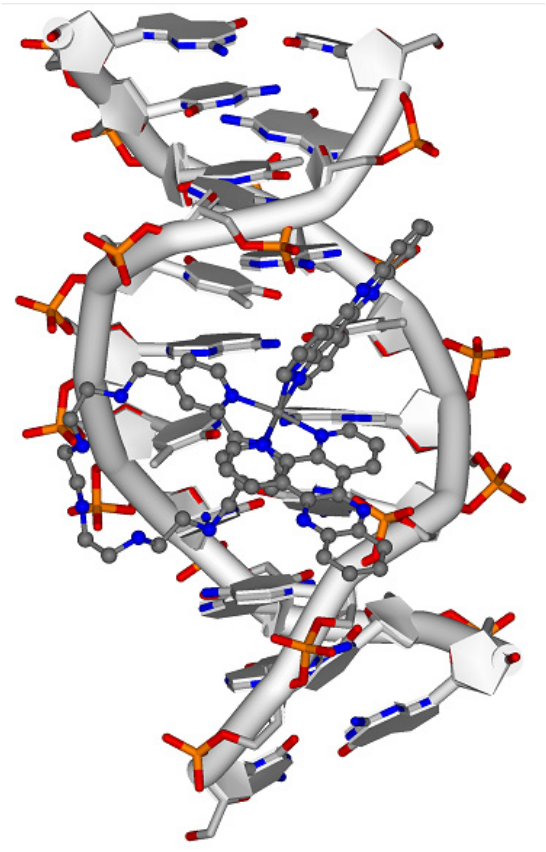

Figure S19. Calculated conformation for the CGCGATATCG/Λ-HD3^{3+} adduct.

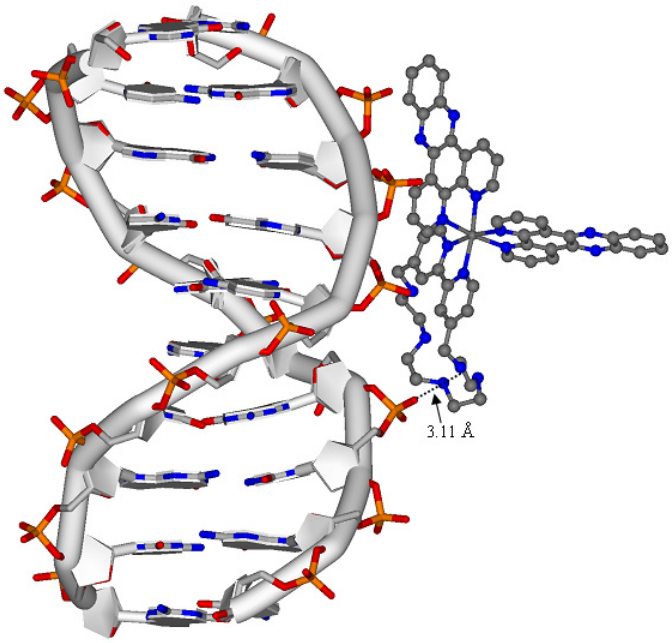

Figure S20. Calculated conformation for the GCGCGCGCGC/Δ-HD3^{3+} adduct.

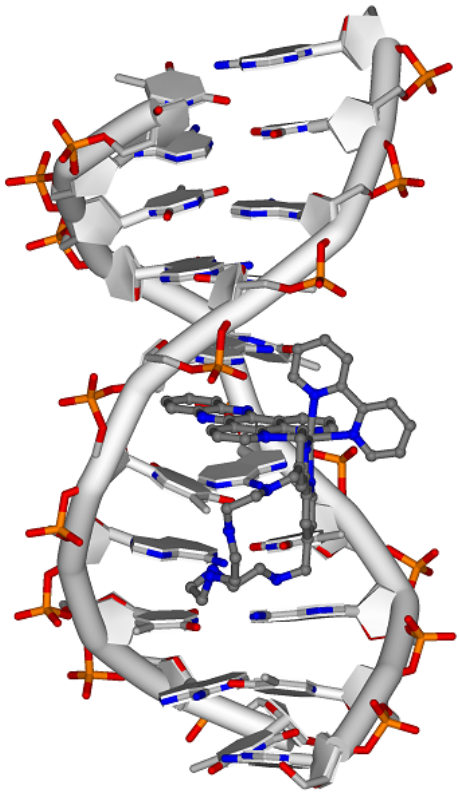

Figure S21. Calculated conformation for the ATATATATAT/Δ-HD2^{3+} adduct.

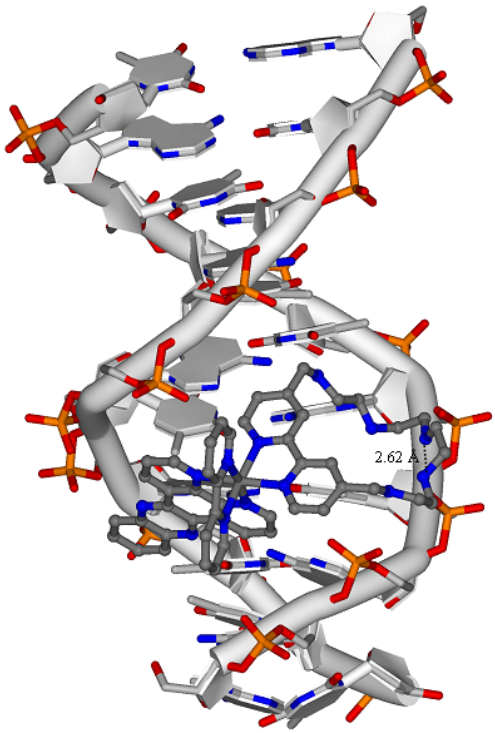

Figure S22. Calculated conformation for the ATATATATAT/Δ-H_2D2^{4+} adduct.

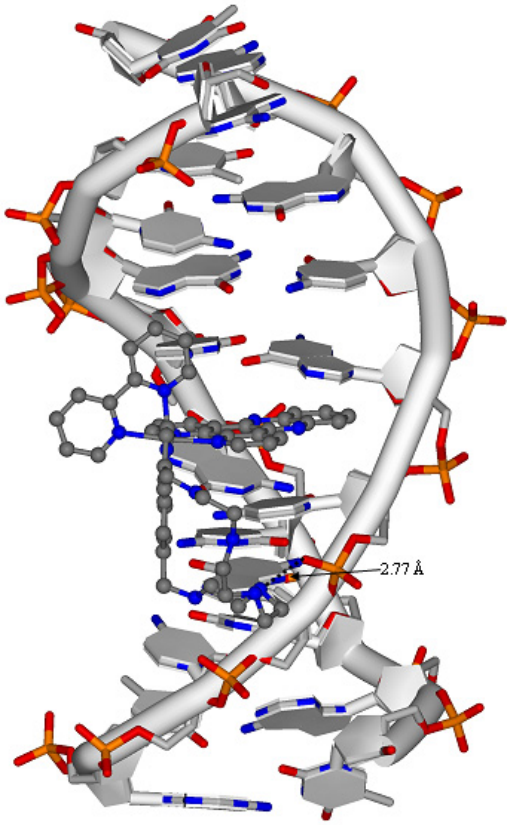

Figure S23. Calculated conformation for the ATCGCGCGAT/Λ-H_2D2^{4+} adduct.

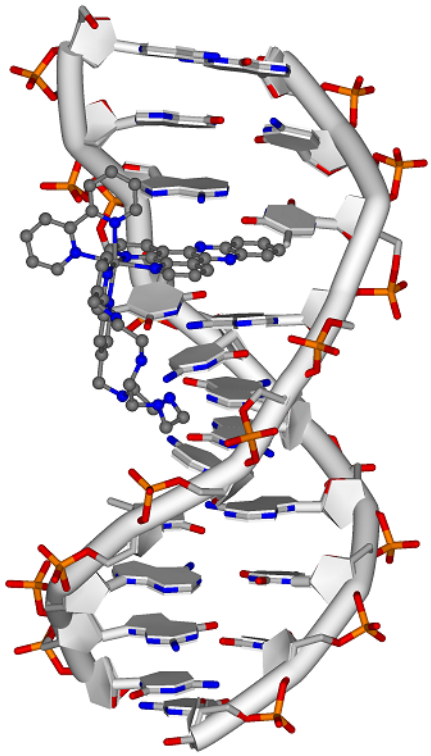

Figure S24. Calculated conformation for the CGATCGATCG/Λ-H_2D2^{4+} adduct.

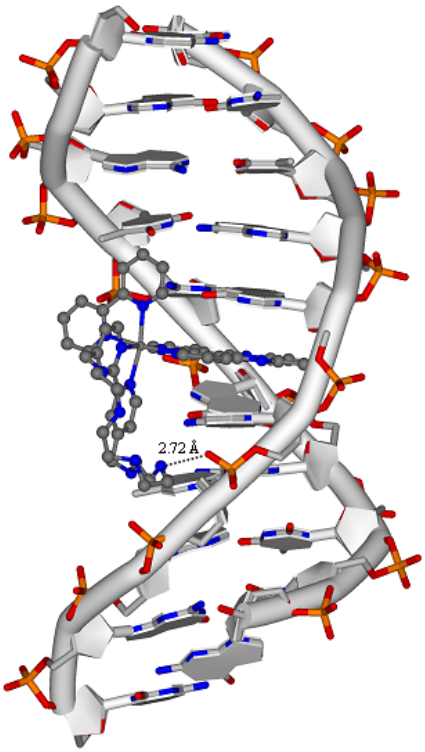

Figure S25. Calculated conformation for the CGATCGATCG/Λ-$HD2^{3+}$ adduct.

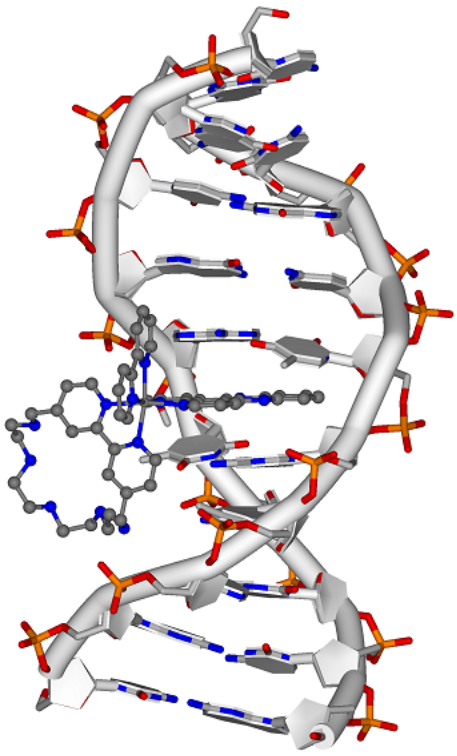

Figure S26. Calculated conformation for the CGCGATATCG/Δ-H_2D2^{4+} adduct.

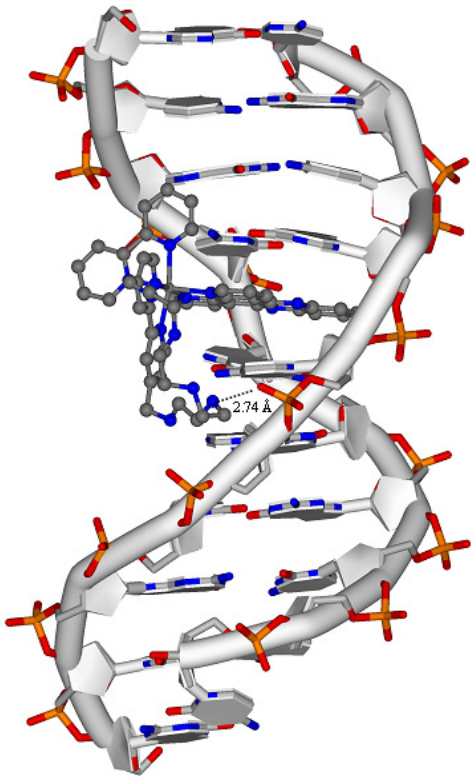

Figure S27. Calculated conformation for the GCGCGCGCGC/Λ-H_2D2^{4+} adduct.